energies

MDPI

Article

How the Chlorine Treatment and the Stoichiometry Influences the Grain Boundary Passivation in Polycrystalline CdTe Thin Films

Alessio Bosio [1], Greta Rosa [1,*], Daniele Menossi [2] and Nicola Romeo [1]

[1] Thin Film Laboratory, Department of Physics and Earth Sciences, University of Parma, Parco area delle Scienze 7/A, Parma 43124, Italy; alessio.bosio@unipr.it (A.B.); nicola.romeo@unipr.it (N.R.)

[2] Computer Science Department, University of Verona, Ca' Vignal 1, Strada Le Grazie 15, Verona 37134, Italy; daniele.menossi@nemo.unipr.it

* Correspondence: greta.rosa@difest.unipr.it; Tel.: +39-0521-905257

Academic Editor: Jean-Michel Nunzi

Received: 21 January 2016; Accepted: 23 March 2016; Published: 31 March 2016

Abstract: The absorption coefficient of CdTe is large enough to assure that all of the visible light is absorbed in a thickness on the order of 1 μm. High efficiency devices are fabricated by using close-spaced sublimation (CSS)-deposited CdTe films with a thickness in the range of 6–8 μm. In order to decrease the thickness of the CdTe film, a novel approach has been used. On top of the CdTe film, whose thickness is reduced to 2–3 μm, another CdTe layer is deposited by RF sputtering, with a thickness of 100–200 nm. The purpose of this approach is to fill up the voids, which tend to form when a low thickness-CdTe film is deposited by close-spaced sublimation. Using this CdTe double layer, solar cells, with an efficiency greater than 15%, were reproducibly obtained. Since the CdTe layer deposited by the CSS technique shows a *p*-type behavior, whereas the layer deposited by sputtering is *n*-type, it is supposed that the formation of a *p*-*n* junction into the grain boundaries, which makes a mirror for the charge carriers, increases their mean lifetime. In order to also have this system after the essential chlorine treatment of the CdTe layer, a special cadmium-free halogen treatment was developed. This process was especially tuned for very thin ($\leqslant$3 μm) CdTe film thickness and for not making use of cadmium-based chlorine salt while, producing high efficiency devices, meets a better economic and environmental sustainability.

Keywords: cadmium telluride; close-spaced sublimation; chlorine treatment; grain boundaries passivation

1. Introduction

In a world with still-increasing global energy demand and forthcoming severe climate changes, the development of sustainable, secure, and competitive energy sources is an issue of topmost priority. The photovoltaic (PV) technology has shown its technical value to contribute significantly to renewable energy sources. Polycrystalline CdTe/CdS thin film solar cells have emerged as a most promising low-cost option for solar cost-effective electricity generation. The advances in CdTe solar cell technology up to now has, to some extent, happened thanks to empirical optimization of a simple device structure in view of achieving a reasonable solar module performance and production yield, but neglecting the material economy and sustainability aspects.

Due to the favorable thermo-physical properties, to a simple phase diagram, and to the chemical stability of the CdTe/CdS solar cell structure, a variety of deposition methods were developed. Different industries and research groups use distinctive techniques for processing CdTe solar cells. Generally, the CdTe deposition method used is taken as a mark of identification of the manufacturer's

technology. Broadly, the CdTe deposition methods can be categorized in "high temperature deposition (HTD)" (⩾770 K), such as close-spaced sublimation (CSS) [1–3], vapor transport deposition (VTD) [4], and atmospheric pressure vapor transport deposition (APVTD) [5], and in "low temperature deposition (LTD)" (⩽670 K), such as high vacuum evaporation (HVE) [6], sputtering [7], spray pyrolysis (SP) [8], and electro-deposition (ED) [9].

It is crucial to recognize the solar cell efficiency dependence on the CdTe growth process, the CdTe layer thickness, the deposition temperature and the substrate type. The most efficient devices are normally grown by the HTD methods, while lower efficiencies are, in general, obtained from LTD techniques, if soda-lime glass is used as a substrate.

Immediately after the CdTe deposition, an annealing treatment of the CdTe/CdS stack is performed in a chlorine atmosphere [10,11] to improve the electronic properties of the absorber layer and of the *p-n* junction. Subsequently the CdTe surface is chemically etched using a "nitric-phosphoric acid" or a "bromine-methanol solution" to create a Te-rich surface that facilitates the formation of an ohmic electrical contact for current transport across the back contact [12–14].

The CdTe layer thickness currently used in high efficiency and stable solar cells and modules is in the range of 3–8 μm depending on the CdTe deposition technique. Thicker absorber layers are employed to avoid pinholes and recombination paths of the charge carriers into the grain boundaries, which have their origin from an incomplete control on film morphology, microstructure, and device architecture. This thickness of the CdTe layer is significantly higher than necessary for optical reasons, as the band gap energy (Eg = 1.45 eV) and the absorption coefficient (>10^4 cm^{-1}) in the visible part of the solar spectrum, suggest that about 1 μm optical thickness (for single passage of photons through the CdTe absorber) and about 0.5 μm physical thickness (with optical reflection to yield high photovoltaic conversion efficiency) are sufficient [15–18].

Although the first generation of CdTe technology is heading towards industrial maturity and has been established as a leading thin film production, it is quite clear that the next generation of CdTe technology needs to address the issues of material resources for consumption and their availability and recycling prospects of multi-gigawatt solar module production in the near future.

The current annual production capacity of tellurium as a byproduct of Cu mining of approximately 2500 metric tons (including the unused Te) will limit the production of CdTe solar modules to about 30×10^9 peak watt (GWp) per year (assuming 15% module efficiency and 5–6 μm CdTe thickness). It is, therefore, obvious that the next generation of CdTe solar cells and modules must be produced with a CdTe layer as thin as possible without losing the overall performance (efficiency and long-term stability). This challenging task can be successfully achieved with a knowledge-driven approach based on in-depth and comprehensive research on the diverse aspects of materials, interfaces, device structures, deposition methods, and processing procedures of advanced CdTe solar modules. The work presented in this article fits this contest: we will explain how a CSS-deposited CdTe layer, with a thickness of only 2–3 μm, leads to a high-efficiency solar cell with a very good over-time stability. In particular, we discovered a new method for the electrical passivation of the grain boundaries and for the pinhole filling, which naturally form when the thickness of the CdTe layer drops well below 5–6 μm. This result was obtained with a particular chlorine treatment of the CdTe/CdS stack without the involvement of $CdCl_2$, nor any other chlorine salt, that allows the deposition of the back contact directly on the just-treated CdTe surface without the use of any chemical etching. In fact, by using HCl as a chlorine supplier, mixed with Ar in the treatment chamber, the CdTe surface is typically Te-rich, as it should be, in order to make a good ohmic contact. The electrical (grain boundaries) and physical (pinholes) passivation is obtained by an additional deposition of a very thin sputtered CdTe film, which show a *n*-type conductivity also after the chlorine treatment. This material, segregating into the grain boundaries of the CdTe film, causes a type-inversion surface, which works as a mirror for the minority carriers. As a result, the grain boundaries, as sources of shunt paths for the photo-generated carriers, are neutralized with a net gain in the junction quality and device time-stability. The use of thin layers of CdTe, together with the chlorine-treatment without the use of toxic substances or acids

for the preparation of the CdTe surface before the realization of the back contact, represents a great benefit into the production chain. The CdTe thickness reduction along with the process robustness as proposed in this article, will have a direct impact on the achievable total annual PV capacity. With only 2 μm of CdTe and an increased efficiency of 16–17%, the total annual CdTe module production can reach 100 GWp per year.

2. Experimental

2.1. The Solar Cell

The structure of the CdTe/CdS superstrate solar cell used for these experiments is shown in [19]. A 6.25 cm square soda-lime glass is covered in sequence by 300 nm thick ITO and 100 nm thick ZnO films, both deposited by sputtering at a substrate temperature of 670 K. After that, the substrate temperature is set at 520 K, at which a 60–80 nm thick CdS film is deposited by RF sputtering in an Ar + 4% CHF_3 (R-23) atmosphere [20]. Subsequently, the substrate temperature is increased up to 770 K and a 2–3 μm thick CdTe film is deposited by close-spaced sublimation (CSS) in an Ar atmosphere with a pressure ranging between 100 Pa and 1000 Pa, with a deposition rate of about 70 nm/s. The CSS system used in these experiments is deeply described in [21]. On top of the CSS-deposited CdTe film, a second CdTe layer, 100–200 nm thick, is deposited by RF sputtering. Then, all the stacked layers are treated at 670 K in a chlorine-containing atmosphere with a new method described in the "the chlorine treatment" session of this paper. Finally, the device is completed by depositing the back-contact, consisting of two layers: a 150 nm thick M_2Te_3 film (M = Sb, As, Bi), covered by a 150 nm thick Mo film [22,23]. These layers are both deposited by DC sputtering.

2.2. Characterization

The electron microscope surface investigations were made with a Zeiss SUPRA® 40 SEM (Oberkochen, Germany) based on a Zeiss GEMINI field emission column. The energy-dispersive X-ray spectroscopy (EDX) measurements were taken by using an Oriel micro-probe equipped with a 10 mm^2 SDD Detector.

A residual gas analyzer (RGA) (MKS CyrrusTM 2 Model, San Jose, CA, USA) was used for the analysis of the process gas during the chlorine treatment of the CdTe film. The mass spectrometer was equipped with a quadrupole capable of measurements in the 1–100 atomic mass unit (amu) range with a detection limit <100 ppb and operational pressure range between 10^5 Pa and 10^{-5} Pa.

Cross-sectional STEM analysis was performed by using a 300 keV Philips CM 300 transmission electron microscope (Amsterdam, The Nederlands) (0.14 nm line resolution for imaging) that is equipped with an Oxford Instruments energy dispersive X-ray system by which line profiles ("depth profiles") can be measured. The resolution of the STEM-EDX analysis is $\leqslant$10 nm.

A continuous LOT-Oriel solar simulator (Irvine, CA, USA), equipped with an air mass (A.M.) 1.5 filter and with a 1 kW/m^2 light power density supplied by a 600 W xenon lamp was used for acquiring the J-V characteristic of the solar cells. A GaAs/AlGaAs solar cell was used as a reference cell and the measurements were made at the standard temperature of 298 K. Short-circuit current density (Jsc) values, not corrected for spectral mismatch, were measured over a calibrated shunt resistor supplied by a Keithley 4200-SCS instrument (Solon, OH, USA).

3. Results and Discussion

3.1. The Chlorine Treatment

An important step in CdTe-based solar cell fabrication is the treatment of the CdTe film in the presence of chlorine, at a temperature of about 670 K. It is generally accepted by the scientific community that the chlorine-treatment increases the grain size of the CdTe film, improves the quality of the grain boundaries and promotes an intermixing of CdS and CdTe layers at their interface. Chlorine

is normally supplied by depositing chlorine salts in the form of thin film on top of the CdTe layer. These salts include $CdCl_2$, $MgCl_2$, NaCl, and NH_4Cl [24–29]. Among them, the Cd-free salts have the great advantage of being much more environmentally sustainable than $CdCl_2$. An alternative way to carry out a Cd-free chlorine treatment of the CdTe film is to use as a halogen carrier gas capable of releasing chlorine or chlorine-containing radicals at the processing temperature. This typology of gases belongs to the chlorine-based Freon family or to the chlorine family itself (HCl, Cl_2, *etc.*). Hydrochloric acid or chlorine are very aggressive gases and their utilization is a cause of instability to the system which makes the CdTe treatment extremely critical [30,31]. Romeo *et al.* in 2006 [32] proposed the alternative approach of using difluoro-chloro-methane (R-22) as the process gas. This treatment provides the same results as those achieved using $CdCl_2$ and solar cells with efficiencies higher than 15% have been produced using this technique. A great advantage of this method is the possibility of controlling the quantity of chlorine-based radicals on the CdTe surface by adjusting the pressure of the treatment atmosphere in the process chamber. Starting from 2011, the industrial utilization of R-22 has been banned in Europe because it is an ozone-depleting substance (ODS). For this reason, other chlorinated hydrocarbon, effective in treating CdTe and not considered ODS, were considered. Possible candidates have been identified among the liquid chlorinated hydrocarbons (LCHY). These materials are liquid at room temperature, easy to handle, and are not subject to any restriction, except for what concerns fire prevention. In the conditions at which treatment takes place, all of these substances are commonly characterized by the presence of hydrochloric acid as part of the LCHY dissociation. HCl itself was investigated as a treatment material and provided very similar results to those obtained with the LCHY. However, the presence of very aggressive species, such as HCl, makes the interaction with the surface of the CdTe film very difficult to control. To ensure a capability to completely control the system, fluorinated hydrocarbons (FLHY) are added to the chlorinated species in the process gas. Using this method, the desired condition for chlorine treatment was obtained and the R-22 results [32] have been easily reproduced. The chlorine treatment is carried out in a quartz ampoule in which the sample is introduced. Firstly, the ampoule is evacuated using a rotary and turbo molecular pump system, reaching a vacuum of at least 1×10^{-4} Pa. Then the ampoule is brought to a temperature between 620 K and 700 K. A controlled amount of chlorinated hydrocarbon is introduced into the ampoule and its pressure is measured through a "baratron"-type head and maintained between 50 Pa and 2×10^3 Pa.

The chlorinated hydrocarbons are liquid and the reaction chamber requires they be delivered in the form of a vapor. The LCHY, kept at room temperature, can be vaporized both by reducing the pressure in the reaction chamber or by passing an inert transporting gas through the LCHY ampoule. The inert gas flux and the pressure in the vaporization chamber must be controlled in order to have the right amount of hydrocarbon in the reaction chamber. The partial vapor pressure of the liquid hydrocarbon depends on the temperature of the vaporizer since it is determined by the liquid-vapor equilibrium. Moreover, a gas of the FLHY family, with partial pressure between 1×10^4 Pa and 4×10^4 Pa, can be mixed with a chlorinated one. An inert gas such as Ar can be added to this mixture of hydrocarbons with partial pressure ranging from 1×10^4 Pa to 4×10^4 Pa in order to reach a maximum total pressure of 5×10^4 Pa. After the CdTe treatment, the gases that exit the quartz ampoule are composed of unreacted species and decomposition fragments. Since these products cannot be released directly into the environment, they must be treated with an abatement process, which releases only the inert transporting gas that can then be recycled. The byproducts of the reaction can be captured by passing them through an alkaline solution.

Among all the possible chlorinated hydrocarbons those that were tested are the following: 1-chlorobutane ($CH_3(CH_2)_3Cl$), 1,1,2-trichloroethylene ($CHClCCl_2$), and dichloromethane (CH_2Cl_2).

When these substances are brought to high temperatures ($\geqslant$650 K), they tend to dissociate into more stable radicals. As Figure 1 clearly highlights, starting with a mixture of Ar and 20% of these hydrocarbons, the molecular species present after one hour of permanence at 670 K are mostly hydrochloric acid ($H^{35}Cl$ and $H^{37}Cl$), while the other molecules detected by the RGA are present in very low quantity, being all below 100 Pa.

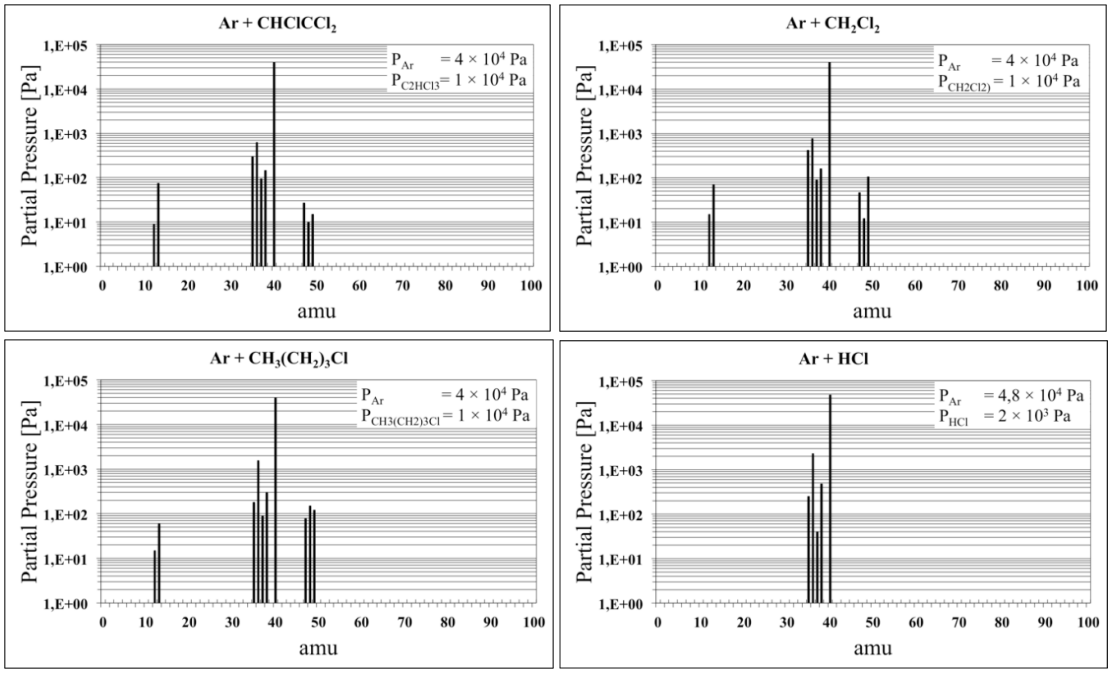

Figure 1. RGA spectra of different LCHYs + Ar and HCl + Ar gas mixtures during the CdTe treatment experiments. Radicals with molecular mass greater than 100 amu are not detected. All of the spectra are taken in the same condition: total pressure = 5 × 10^4 Pa, temperature = 670 K, time = 1 h. For line recognition please refer to Table 1.

Table 1. Some dissociation products of the chlorinated and fluorinated hydrocarbons at a fixed temperature of 670 K. These data, in atomic mass unit (amu), were taken from [33].

Product of Dissociation							
Substance	**Amu**	**Substance**	**Amu**	**Substance**	**Amu**	**Substance**	**Amu**
C(n)	12	^{35}Cl(n)	35	HF_2(i)	39	CH_2Cl(i)	49
CH(i)	13	H^{35}Cl(n)/^{36}Ar(n)	36	^{4}Ar(n)	40	CHF_2(i)	51
CH2F(i)	31	^{37}Cl(n)	37	CCl(i)	47	CF^{35}Cl(i)	66
CH_2F(i)	33	H^{37}Cl(i)	38	CHCl(i)	48	C_2F_4(n)	100
(n) = neutral; (i) = ionic							

These spectra, recorded every 30 s during the treatment, show that the dissociation of the Freon molecules is a rather slow process: a rapid heating of the gas to 670 K will not ensure that all the Freon gas is dissociated. From this dynamic measurement, rough estimates were made, which indicate that only 3% to 6% of the Freon dissociates during the first 5 min and this dissociation rate remains fairly constant.

The steady state condition can be reached only if dissociation and recombination rates are the same, and this is strictly true if the quantity of Freon is fixed and the treatment temperature is 670 K. In order to perform the CdTe treatment in a steady state condition, only time periods of at least 10 min were used. At higher temperatures the products of dissociation are different, often involving the double bond between two carbon atoms. When these compounds are formed, the reaction is no longer reversible, and all of the Freon present will then dissociate; for example, at a temperature of 800 K all the tested freons are completely dissociated after 5 min.

Figure 1 shows that the treatment is always carried out in presence of hydrochloric acid as the RGA measurement confirms. In these conditions, since the reactivity is very high, the system becomes critical and the results, summarized in Table 2, show that the efficiencies of the cells produced are

lower than 10%. This critical condition, due to excessive reactivity, is also highlighted by the standard deviation of the photovoltaic parameters, which is always more than three times the standard deviation normally obtained using the reference treatment with R-22.

Table 2. Treatment condition of the CdTe film in the presence of different liquid chlorinated hydrocarbons (LCHYs) with corresponding photovoltaic and diode parameters of the completed cells.

Treatment Conditions				Photovoltaic and Diode Parameters			
Temperature [K]	Pressure [Pa] LCHY	Pressure [Pa] Ar	Time [min]	Nr of Cells	Rs * [ohm]	Rsh * [ohm]	Efficiency [%]
CHClCCl2 (1,1,2-Trichloroethylene)							
673	200	4.98 × 104	15	25	1.8 ± 0.9	87 ± 11	9.3 ± 1.1
	500	4.95 × 104	10	19	1.5 ± 0.4	59 ± 9.3	5.7 ± 1.7
CH2Cl2 (Dichloromethane)							
673	100	4.99 × 104	15	25	2.2 ± 0.9	82 ± 9.9	8.8 ± 0.9
	500	4.95 × 104	10	22	1.1 ± 0.6	63 ± 8.7	6.5 ± 1.5
CH3(CH2)3Cl (1-Chlorobutane)							
673	200	4.98 × 104	15	20	1.8 ± 1.1	77 ±12	7.8 ± 1.4
	500	4.95 × 104	10	23	0.9 ± 0.5	58 ± 11	5.4 ± 2.2

* Series (R_s) and shunt (R_{sh}) resistances, referred to solar cells with an area of 1 cm^2, are extrapolated from the under light J-V characteristics.

Now we have to answer to the following question: what is the main difference between LCHYs and R-22 from the CdTe treatment point of view? Up to now, we considered only the CdTe-Cl_2 interaction, but R-22 carries F_2 and/or F-based species with a probable formation of a fluorine compound. Some of these are stable materials at the treatment temperature, but in presence of chlorine they could present a metastable phase. The formation of fluorine compounds, such as CdF_2, is effective in lowering the formation rate of the chlorine containing counterparts ($CdCl_2$), decreasing the chlorine aggressiveness and making the system easier to control. In order to align the LCHY treatment as much as possible to what is achieved using the R-22 system, chlorine-free fluorinated hydrocarbons were supplied into the treatment chamber. This solution provides an additional knob for controlling the process, *i.e.* adjusting the partial pressure of the FLHY to fine-tune the reactivity of the species containing chlorine. This method, being able to vary the amount of chlorine- and fluorine-containing species by independently managing the LCHY and FLHY partial pressures, proved to be even more effective than the R-22-based treatment.

Actually, the etching effect of the CdTe surface, typical of films treated with the LCHYs alone, decreases by increasing the quantity of fluorine in the treatment gas. As a consequence, the grain boundaries of the CdTe film are less carved and the chlorine action in the junction region is soft enough to passivate the structural defects, promoting the formation of an intermixing layer [22] without destroying the interface between CdTe and CdS.

The FLHY species considered are the ones listed in Table 3 and among them, those actually tested are: trifluoromethane R-23 (CHF_3), R-134a (1,1,1,2-tetrafluoroethane, CH_2FCF_3), and R-152a (1,1-difluoroethane, CH_3CHF_2). These fluorinated hydrocarbons are commonly used in refrigeration and are readily available. Furthermore, since hydrochloric acid is always present among the dissociation products of all the examined LCHYs, (see Figure 1) the Ar + HCl + FLHY system was also tested. Figure 2 shows the morphology of a CSS-deposited CdTe film, 6 μm thick, as it appears, Figure 2a, as deposited, and Figure 2b,c after the Ar + R-22 and the Ar + HCl + R-23 processing, respectively. The treatment conditions are reported in Figure 3.

The morphology of the surfaces shown in Figure 2b,c presents the typical mesa-like structure resulting from the etching of the surface by chlorine and/or hydrogen chloride.

The crystalline grains tend to coalescence, becoming more compact with narrow boundaries.

Table 3. Fluorinated hydrocarbons suitable for the fine-tuning of the chlorine reactivity during the CdTe film treatment.

Fluorinated Hydrocarbons					
Trade Name	**Name**	**Chemical Formula**	**Trade Name**	**Name**	**Chemical Formula**
R-23	Trifluoromethane	CHF_3	R-32	Difluoromethane	CH_2F_2
R-125	Pentafluoroethane	CHF_2CF_3	R-134a	1,1,1,2-Tetrafluorethane	CH_2FCF_3
R-143a	1,1,1-Trifluoroethane	CH_3CF_3	R-152a	1,1-Difluoroethane	CH_3CHF_2

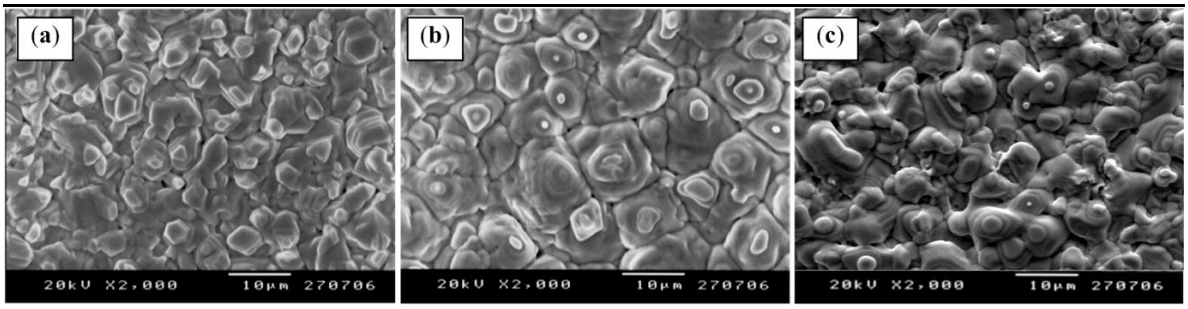

Figure 2. SEM images of CdTe film morphology (**a**) before, and (**b**,**c**) after chlorine-treatment with Ar + R-22 and with Ar + HCl + R-23 respectively.

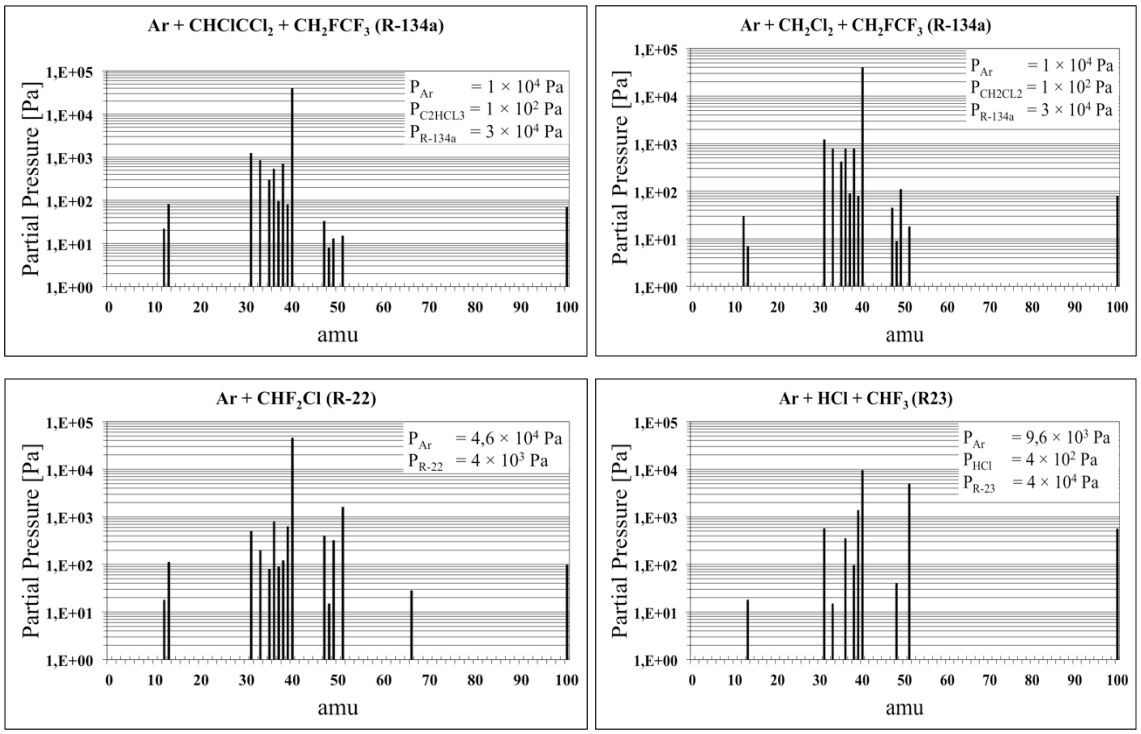

Figure 3. RGA spectra of different LCHY + FLHY + Ar gas mixtures during the CdTe treatment experiments. Radicals with molecular mass larger than 100 amu are not detected. All of the spectra are taken in the same condition: total pressure = 5×10^4 Pa, temperature = 670 K, time = 1 h. For line recognition please refer to Table 1.

Moreover, the formation of micro-particles of carbon on the surface of the CdTe, which occurs when using only the chlorinated compound, is inhibited, probably because the fluorine-containing gas tends to bond the carbon atoms. In Figure 3, the RGA measurements concerning the

$CHClCCl_2$ + R-134a + Ar, CH_2Cl_2 + R-134a + Ar, and the HCl + R-23 + Ar gas mixtures are compared to what is observed with the R-22 + Ar system.

These experiments conclusively show that the CdTe treatment, using liquid chlorinated hydrocarbons, can produce similar results to those achieved using the R-22 system if chlorine-free fluorinated hydrocarbons are added in the reaction chamber to control the chlorine reactivity.

The behavior of the solar cells built with CdTe films treated with the LCHY + FLHY gas mixture confirms the above observations. The treatment time for these samples was 15 min, whereas the trials referred to in Figure 3 had treatment durations of one hour. The properties of the photovoltaic cells produced using these treatments are presented in Table 4. The efficiency of these devices is quite high, showing that the diode parameters of the devices are very good. The low standard deviation of all the parameters suggests high reproducibility, which means the chlorine treatment, exploiting the LCHY and Ar gas mixture to which FLHY has been added, is completely under control. As the back contact is not contaminated by carbon filaments, which are present if the chlorinated hydrocarbon is used alone, a very good time stability of the solar cell is expected. In fact, CdTe solar cells, kept under one sun at 353 K (accelerated lifetime test) in a metal box, show a very stable behavior exhibiting, after 1300 h, an efficiency of more than 93% of the initial performance.

Table 4. Photovoltaic and diode behavior of finished solar cells in which the CdTe layer was treated with the special gas mixtures reported in Figure 3.

Photovoltaic and Diode Parameters				
Gas Mixture	**Nr of Cells**	**R_s * [ohm]**	**R_{sh} * [ohm]**	**Efficiency [%]**
Ar + $CHClCCl_2$ + R-134a	23	1.2 ± 0.02	1657 ± 20	15.7 ± 0.5
Ar + CH_2Cl_2 + R-134a	32	1.5 ± 0.04	1550 ± 9	14.6 ± 0.5
Ar + R-22	50	0.8 ± 0.01	1870 ± 5	15.8 ± 0.3
Ar + HCl + R23	50	1.1 ± 0.01	1900 ± 5	16.2 ± 0.2

* Series (R_s) and shunt (R_{sh}) resistances, referred to solar cells with an area of 1 cm^2, are extrapolated from the under light J-V characteristics.

3.2. Pinholes and Grain Boundaries Passivation

Up to now, we always considered CdTe films with thickness greater than 6 µm, which corresponds to a standard for this CSS-deposited film (Figure 4b). What happens if the thickness is reduced to a third of the standard (Figure 4a)? The crystalline grains are reduced in size, highlighting widened grain boundaries with some voids, which favor the formation of shunt-paths and, therefore, of weak *p-n* junctions. As a result, lower photovoltages and fill factors are obtained.

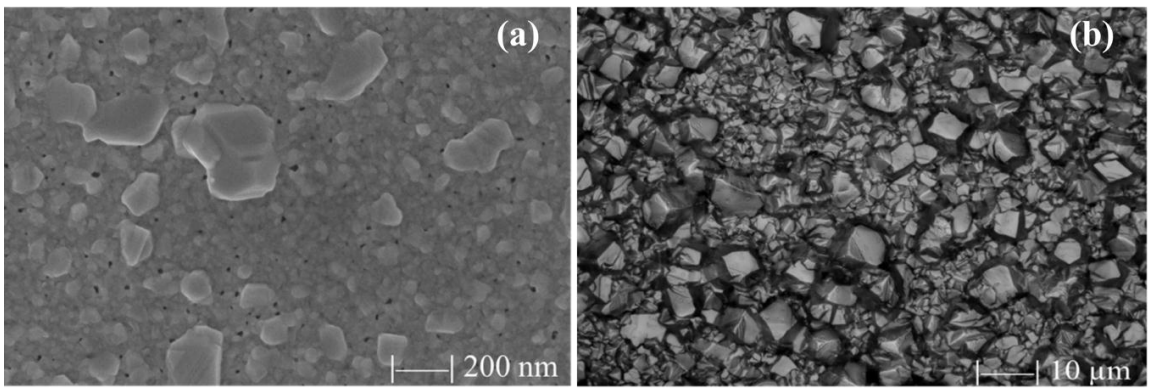

Figure 4. SEM images of the surface morphology of CSS-deposited film: (**a**) 2 µm thick CdTe layer; the black points in the picture correspond to holes probably due to an incomplete coalescence of the CdTe grains; and (**b**) 6 µm thick CdTe layer.

From a stoichiometry point of view, there is no difference between thicker or thinner films if CdTe is deposited by CSS; in both cases the CdTe layer exhibits a Te-rich surface as shown by SEM-EDX measurements performed on a CSS-deposited film (Figure 5a). Making the chlorine treatment by using HCl, LCHY, and by adding FLHYs, offers a great advantage since the CdTe surface continues to be Te-rich after the treatment; the peculiarity is that this treatment does not introduce Cd into the CdTe film from outside leaving the Cd-vacancies un-compensated (Figure 5b); this fact does not happen if a cadmium salt like $CdCl_2$ is used. During this study, we discovered this important feature, which could be exploited by making the back-contact directly on the surface of the CdTe layer. In fact, it is commonly accepted by the research community that, in order to obtain a good ohmic contact with *p*-type CdTe, a Te-rich surface is needed.

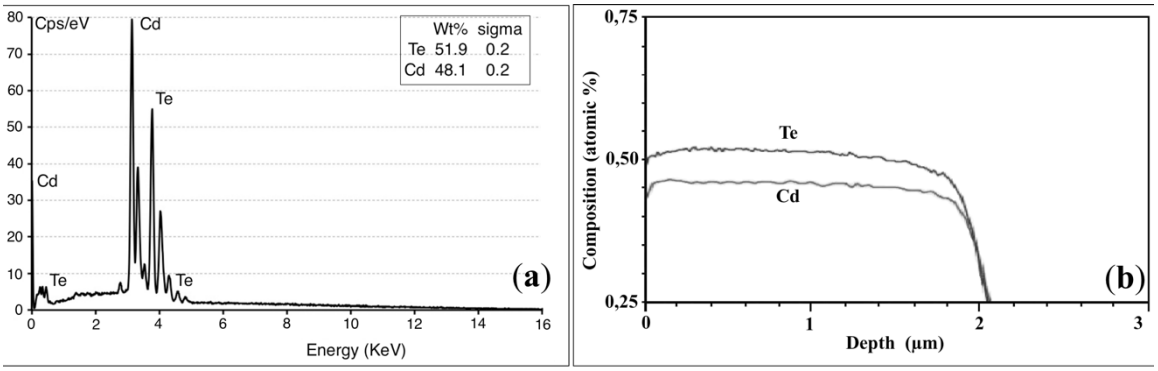

Figure 5. Stoichiometry of a CSS-deposited CdTe film: (**a**) EDX measurement showing the weight percentages of Te (51.9%) and Cd (48.1%); and (**b**) SIMS measurement performed on the first 2 µm close to the surface film.

On the contrary, sputtered CdTe films, being deposited at a lower temperature (<623 K) if compared with those deposited with the CSS technique (>770 K), are very compact with an excellent coverage already at very low thickness and completely hole-free (Figure 6a). Moreover, CdTe films deposited by RF sputtering in a pure Ar atmosphere at a temperature around 570 K show a Cd-rich stoichiometry. Furthermore, these films exhibit a resistivity of about 1×10^3 Ωcm with a *n*-type behavior, presumably due to the Te-vacancies as the Cd/Te ratio suggest (Figure 6b), despite the starting material has a purity of 99.999% with a Cd/Te ratio $R_{Cd/Te} = 1$.

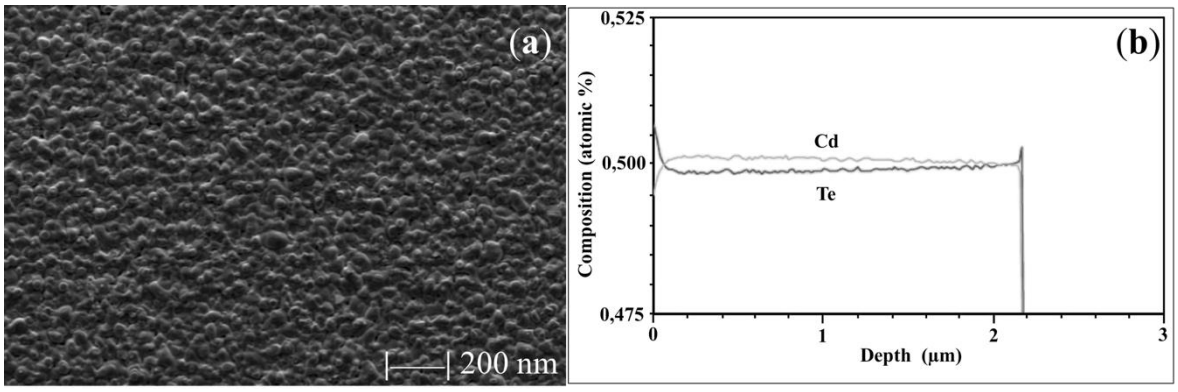

Figure 6. (**a**) SEM image of the surface of a CdTe film deposited by RF sputtering with a thickness of 200 nm before the typical Cl-treatment; and (**b**) SIMS measurement put in evidence the Cd-rich nature of the CdTe film also after the Cl-treatment.

Since the decrease of the CdTe film thickness will become increasingly mandatory in the near future, we tried to fill in the holes of a 3 μm thick CSS-CdTe film with a 100–200 nm thick sputtered-CdTe film. This bi-layer was treated at a temperature of 670 K in HCl + FLHY + Ar gas mixture and then the resulting solar cell was completed by depositing the standard back-contact.

The obtained solar cell exhibits open circuit voltage Voc ≈ 830 mV, short circuit current density Jsc ≈ 25–26 mA/cm^2, fill factor FF ≈ 0.70 and efficiencies Eff ≈ 15% as it is shown in Figure 7 and summarized in Table 5. In order to explain this results an ad hoc hypothesis was made: at the back-contact side, of a CSS as-deposited polycrystalline CdTe film, the grain boundaries (GBs) act as electron traps, while rejecting holes. After the chlorine treatment the GBs have sufficiently strong, localized Cl segregation (n-type levels) to cause the formation of a p-n-p junction across the GB. The built-in field, formed in the regions between the GB and grain interior, will act as a mirror for the minority carrier and will help separate photo-generated carriers reducing the carrier recombination rate.

Table 5. Photovoltaic parameters of three CdTe-based solar cells, whose characteristics are reported in Figure 7. Only the #5333 sample is related to a solar cell made with a CdTe bi-layer.

Sample	Voc (mV)	Jsc (mA)	FF (%)	Eff. (%)	R_s * [ohm]	R_{sh} * [ohm]
# 5333	830	25.2	70.01	14.94	5.6 ± 0.02	1428 ± 20
# 5591	860	26.1	59.2	13.19	10.6 ± 0.04	1250 ± 9
# 5561	786	24.5	50.4	9.36	14.2 ± 0.01	227 ± 5

* Series (R_s) and shunt (R_{sh}) resistances, referred to solar cells with an area of 1 cm^2, are extrapolated from the under light J-V characteristics.

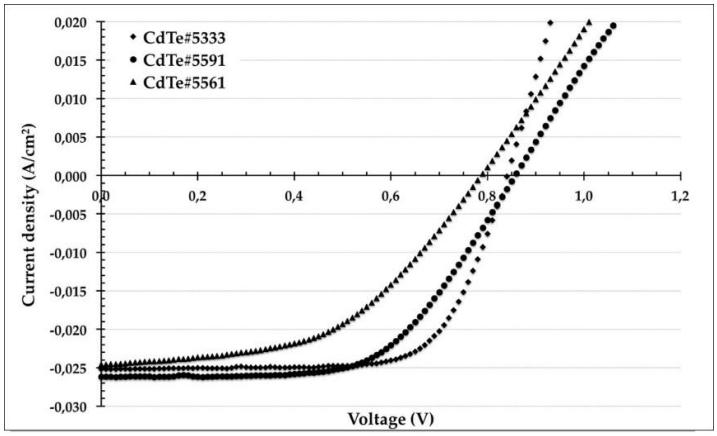

Figure 7. Comparison between the J-V characteristics of three different solar cells: #5333 concerns a 3 μm thick CSS-CdTe film, covered by 200 nm thick layer of a sputtered-CdTe film, #5991 concerns a 8 μm thick CSS-CdTe film and #5561 concerns a 3 μm thick CSS-CdTe film. All these three solar cells are made in the same way, except for the CdTe film.

This effect is well explained by Li *et al.* in [34]. Moreover, we increase this multiple effect by using a very thin n-type CdTe layer, which is segregated into the GBs of the p-type CSS-deposited CdTe underneath layer after the chlorine treatment. The resulting *p-n* junction, formed between the grain boundaries and the bulk, could reject the minority carriers inside the grain increasing their lifetime.

This active passivation of the grain boundaries is effective also against the formations of shunt paths, only if the the bottom of the hole does not completely leave uncovered the buffer layer (CdS) and this is true only when the thicknesses of the CSS-CdTe layer are ⩾2 μm. This hypothesis is confirmed by the STEM-EDX analysis performed on a CdTe bilayer immediately after the chlorine-treatment as it is shown in Figure 8 and in Table 6.

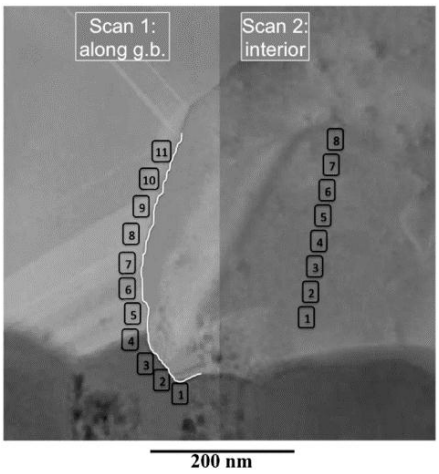

Figure 8. The stoichiometry of the grain-boundary (left sequence) and of the grain-surface (right sequence) was measured by energy-dispersive X-ray analysis (EDX) using a scanning transmission electron microscope (STEM). The values of this measurement are listed in Table 6.

Table 6. Atomic % concentrations of S, Cl, Cd, and Te both inside the grain boundaries (left) and into the grains (right) of a CdTe-bilayer/CdS stack after chlorine treatment.

EDX Scan Along Grain Boundary					EDX Scan Inside Grain			
#	S	Cl	Cd	Te	#	S	Cd	Te
1	29.3	4.9	42.4	23.4	1	4.4	46.2	49.4
2	16.1	4.8	35.0	44.1	2	3.2	47.3	49.5
3	24.4	4.0	45.4	26.2	3	2.1	48.2	49.7
4	17.1	5.1	44.7	33.1	4	3.0	47.3	49.7
5	3.2		47.7	49.1	5	2.3	47.8	49.8
6	2.9		50.7	46.4	6		48.5	51.5
7	2.9		49.3	47.8	7		51.2	48.8
8	2.5		49.4	48.1	8		51.3	48.7
9	2.8		49.7	47.5				
10	3.0		49.2	47.8				
11	2.7		50.8	46.5				

4. Conclusions

The PV module production based on CdTe technology will increasingly have to deal with the supply of rare elements such as tellurium. The work presented in this article assumes a reduction of the thickness of the absorber layer in order to meet this requirement. The use of CdTe thin layers, 2–3 μm thick, is generally prevented by the formation of pinholes into the CSS-deposited films. We proved that this difficulty can be overcome by the deposition of a sputtered-CdTe film, 200 nm thick, on top of the CSS-CdTe layer. We discovered that the CSS-deposited CdTe film is Te-rich, while the sputtered one exhibits a Cd-rich stoichiometry with a *n*-type conductivity. After the chlorine-treatment the Cd-rich material is confined into the grain-boundaries of the CSS-deposited film giving rise to an inversion-type layer, which acts as a mirror for the minority carriers increasing their lifetime and preventing the formation of shunt paths. This is made possible by a particular chlorine-treatment of the CdTe bi-layer especially devised for this purpose. The Cl-treatment is made by using a mixture of liquid chlorinated hydrocarbons or Ar + HCl added with fluorinated hydrocarbons instead of the usual inorganic chlorine salts. This Cd-free treatment, as well as being more environmentally sustainable, does not introduce cadmium atoms from the outside, leaving the surface of the CdTe crystal grains Te-rich, ready to make a good ohmic contact. In conclusion, this specific process leads to the realization of polycrystalline CdTe thin film solar cells, which exhibit efficiencies above 15%, while using a total thickness of the absorber layer of $\leqslant$3 μm.

Author Contributions: Alessio Bosio growth, deposition and heat-treatment equipment design and installation, sputtering target preparation, project coordination; Greta Rosa and Daniele Menossi sputtering deposition and materials characterization, device modelling and processing; Nicola Romeo chlorine treatment, electrical characterization, lab coordination.

Conflicts of Interest: The authors declare no conflict of interest.

References

1. Bonnet, D.; Rabenhorst, H. New results on the development of thin film p-CdTe/n-CdS hetero-junction solar cells. In Proceedings of the 9th Photovoltaic Specialists Conference, New York, NY, USA, 1972; pp. 129–131.
2. Ferekides, C.; Britt, J.; Ma, Y.; Killian, L. High efficiency CdTe solar cells by close spaced sublimation. In Proceedings of the 20th IEEE Photovoltaic Specialists Conference, Louisville, KY, USA, 10–14 May 1993; pp. 389–393.
3. Chu, T.L.; Chu, S.S.; Ferekides, C.; Wu, C.Q.; Britt, J.; Wang, C. 13.4% efficient thin-film CdS/CdTe solar cells. *J. Appl. Phys.* **1991**, *70*, 7608–7612. [CrossRef]
4. Hanket, G.M.; McCandless, B.E.; Buchanan, W.A.; Fields, S.; Birkmire, R.W. Design of a vapor transport deposition process for thin film materials. *J. Vac. Sci.Tech. A* **2006**, *24*, 1695–1701. [CrossRef]
5. Meyers, P.V.; Kee, R.J.; Raja, L.; Wolden, C.A.; Aire, M. Atmospheric pressure chemical vapor deposition of CdTe-reactor design considerations. In Proceedings of the 15th AIP National Center for Photovoltaics (NCPV) Program Review Meeting, Denver, CO, USA, 9–11 September 1998; pp. 218–223.
6. Romeo, A.; Buecheler, S.; Giarola, M.; Mariotto, G.; Tiwari, A.N.; Romeo, N.; Bosio, A.; Mazzamuto, S. Study of CSS- and HVE-CdTe by different recrystallization processes. *Thin Solid Films* **2009**, *517*, 2132–2135. [CrossRef]
7. Shao, M.; Fischer, A.; Grecu, D.; Jayamaha, U.; Bykov, E.; Contreras-Puente, G.; Bohn, R.G.; Compaan, A.D. Radio-frequency-magnetron-sputtered CdS/CdTe solar cells on soda-lime glass. *Appl. Phys. Lett.* **1996**, *69*, 3045–3047. [CrossRef]
8. Ma, Y.Y.; Fahrenbruch, A.L.; Bube, R.H. Photovoltaic properties of n-cadmium sulfide/p-cadmium telluride hetero-junctions prepared by spray pyrolysis. *Appl. Phys. Lett.* **1977**, *30*, 423–424. [CrossRef]
9. Panicker, M.P.R.; Knaster, M.; Kröger, F.A. Cathodic deposition of CdTe from aqueous electrolytes. *J. Electrochem. Soc.* **1978**, *125*, 566–572. [CrossRef]
10. Ferekides, C.; Marinskiy, D.; Morel, D.L. CdS: Characterization and recent advances in CdTe solar cell performance. In Proceedings of the 26th IEEE Photovoltaic Specialists Conference, Anaheim, CA, USA, 29 September–3 October 1997; pp. 339–342.
11. Mazzamuto, S.; Vaillant, L.; Bosio, A.; Romeo, N.; Armani, N.; Salviati, G. A study of the CdTe treatment with a Freon gas such as CHF2Cl. *Thin Solid Films* **2008**, *516*, 7079–7083. [CrossRef]
12. Dobson, K.D.; Visoly-Fisher, I.; Hodes, G.; Cahen, D. Stability of CdTe/CdS thin-film solar cells. *Sol. Energy Mater. Sol. Cells* **2000**, *62*, 295–325. [CrossRef]
13. Durose, K.; Edwards, P.R.; Halliday, D.P. Materials aspects of CdTe/CdS solar cells. *J. Cryst. Growth* **1999**, *197*, 733–742. [CrossRef]
14. Romeo, N.; Bosio, A.; Tedeschi, R.; Romeo, A.; Canevari, V. A highly efficient and stable CdTe/CdS thin film solar cell. *Sol. Energy Mater. Sol. Cells* **1999**, *58*, 209–218. [CrossRef]
15. Mitchell, K.; Fahrenbruch, A.L.; Bube, R.H. Photovoltaic determination of optical-absorption coefficient in CdTe. *J. App. Phy.* **1977**, *48*, 829–830. [CrossRef]
16. Mykytyuk, T.I.; Rosko, V.Y.; Kosyachenko, L.A. Limitations on thickness of absorber layer in CdS/CdTe solar cells. *Acta Phy. Pol. A* **2012**, *122*, 1073–1076. [CrossRef]
17. Morales-Acevedo, A. Design of very thin CdTe solar cells with high efficiency. *Energy Proced.* **2014**, *57*, 3051–3057. [CrossRef]
18. Paudel, N.R.; Wieland, K.A.; Young, M.; Asher, S.; Compaan, A.D. Stability of sub-micron-thick CdTe solar cells. *Prog. Photovolt. Res. Appl.* **2014**, *22*, 107–114. [CrossRef]
19. Bosio, A.; Romeo, N.; Menossi, D.; Rosa, G.; Lottici, P.P.; Romeo, A.; Rimmaudo, I.; Salavei, A. Key developments in CdTe thin film solar cell back-contact. In Proceedings of the 28th European Photovoltaic Solar Energy Conferenceand Exhibition (EUPVSEC), Paris, France, 30 September–4 October 2013; pp. 2357–2361.

20. Podestà, A.; Armani, N.; Salviati, G.; Romeo, N.; Bosio, A.; Prato, M. Influence of the Fluorine doping on the optical properties of CdS thin films for photovoltaic applications. *Thin Solid Films* **2006**, *511–512*, 448–452. [CrossRef]
21. Bosio, A.; Romeo, N.; Mazzamuto, S.; Canevari, V. Polycrystalline CdTe thin films for photovoltaic applications. *Prog. Cryst. Growth Charact. Mater.* **2006**, *52*, 247–279. [CrossRef]
22. Romeo, N.; Bosio, A.; Canevari, V.; Podestà, A.; Mazzamuto, S.; Guadalupi, G.M. High efficiency CdTe/CdS thin film solar cells with Sb2Te3 back contact by a thoroughly dry process. In Proceedings of the 19th European Photovoltaic Solar Energy Conferenceand Exhibition (EUPVSEC), Paris, France, 7–11 June 2004; pp. 1718–1720.
23. Romeo, A.; Salavei, A.; Rimmaudo, I.; Bosio, A.; Menossi, D.; Piccinelli, F.; Romeo, N. Electrical characterization and aging of CdTe thin film solar cells with Bi2Te3 back contact. In Proceedings of the 39th IEEE Photovoltaic Specialists Conference, Tampa, FL, USA, 16–21 June 2013; pp. 1178–1182.
24. Bayhan, H. Investigation of the effect of $CdCl_2$ processing on vacuum deposited CdS/CdTe thin film solar cells by DLTS. *J. Phy. Chem. Solids* **2004**, *65*, 1817–1822. [CrossRef]
25. Hiie, J. CdTe:CdCl2:O2 annealing process. *Thin Solid Films* **2003**, *431–432*, 90–93. [CrossRef]
26. Niles, D.W.; Waters, D.; Rose, D. Chemical reactivity of $CdCl_2$ wet-deposited on CdTe films studied by X-ray photoelectron spectroscopy. *Appl. Surf. Sci.* **1998**, *136*, 221–229. [CrossRef]
27. Williams, L.B.; Major, J.D.; Bowen, L.; Keuning, W.; Creatore, M.; Durose, K. A Comparative Study of the Effects of Nontoxic Chloride Treatments on CdTe Solar Cell Microstructure and Stoichiometry. *Adv. Energy Mater.* **2015**, *5*, 1500554–1500563. [CrossRef]
28. Potlog, T.; Ghimpu, L.; Gashin, P.; Pudov, A.; Nagle, T.; Sites, J. Influence of annealing in different chlorides on the photovoltaic parameters of CdS/CdTe solar cells. *Sol. Energy Mater. Sol. Cells* **2003**, *80*, 327–334. [CrossRef]
29. Potter, M.D.G.; Halliday, D.P.; Cousins, M.; Durose, K. A study of the effects of varying cadmium chloride treatment on the luminescent properties of CdTe/CdS thin solar cells. *Thin Solid Films* **2000**, *361–362*, 248–252. [CrossRef]
30. Zhou, T.X.; Reiter, N.; Powell, R.C.; Sasala, R.; Meyers, P.V. Vapor chloride treatment of polycrystalline CdTe/CdS films. In Proceedings of the 1st IEEE Photovoltaic Specialists Conference, Waikoloa, HI, USA, 5–9 December 1994; pp. 103–106.
31. Qu, Y.; Meyers, P.V.; Mc Candless, B.E. HCl vapor post-deposition heat treatment of CdTe/CdS films. In Proceedings of the 25th IEEE Photovoltaic Specialists Conference, Washington, DC, USA, 13–17 May 1996; pp. 1013–1016.
32. Romeo, N.; Bosio, A.; Romeo, A.; Mazzamuto, S. High Efficiency CdTe/CdS Thin Film Solar Cells Prepared by Treating CdTe Films with a Freon Gas in Substitution of CdCl2. In Proceedings of the 21th European Photovoltaic Solar Energy Conferenceand Exhibition (EUPVSEC), Dresden, Germany, 4–8 September 2006; pp. 1857–1860.
33. Search for Species Data by Molecular Weight. Available online: http://webbook.nist.gov/chemistry/mw-ser.html (accessed on 24 March 2016).
34. Li, C.; Wu, Y.; Poplawsky, J.; Pennycook, T.J.; Paudel, N.; Yin, W.; Haigh, S.J.; Oxley, M.P.; Lupini, A.R.; Al-Jassim, M.; *et al*. Grain-Boundary-Enhanced Carrier Collection in CdTe Solar Cells. *Phy. Rev. Lett.* **2014**, *112*. [CrossRef] [PubMed]